High Mobility of Bicoid Captured by Fluorescence Correlation Spectroscopy: Implication for the Rapid Establishment of Its Gradient

Asmahan Abu-Arish,[†] Aude Porcher,[§¶] Anna Czerwonka,[†] Nathalie Dostatni,[§¶] and Cécile Fradin[†‡*]

[†]Department of Physics and Astronomy, and [‡]Department of Biochemistry and Biomedical Sciences, McMaster University, Hamilton, Ontario, Canada; [§]Institut Curie, Centre de Recherche, Paris, France; and [¶]Institut Curie, Centre de Recherche, Centre National de la Recherche Scientifique, UMR 218, Paris, France

ABSTRACT The Bicoid (Bcd) morphogen is essential for pattern formation in fruit flies. It forms an exponential concentration gradient along the embryo AP axis and turns on cascades of target genes in distinct anterior domains. The most commonly accepted model for gradient formation assumes that Bcd travels by simple diffusion and is uniformly degraded across syncytial embryos, yet several recent studies have challenged these ideas. Here, the question of Bcd mobility was investigated using fluorescence correlation spectroscopy in live *Drosophila melanogaster* embryos. Bcd-EGFP molecules were found to be highly mobile in the cytoplasm during cycles 12–14, with a diffusion coefficient ~7 $\mu m^2/s$. This value is large enough to explain the stable establishment of the Bcd gradient simply by diffusion before cycle 8, i.e., before the onset of zygotic transcription.

Received for publication 2 March 2010 and in final form 17 May 2010.

*Correspondence: fradin@physics.mcmaster.ca

The development of axial polarities is generally controlled by morphogenetic gradients, which instruct cell fate in a concentration- or activity-dependent manner (1). Understanding how these gradients are established is essential to appreciate the precision and robustness of their associated transcriptional response (2–4). In fruit flies, the 54-kDa Bicoid (Bcd) protein is the primary determinant of cell differentiation along the anterior-posterior (AP) axis. It was one of the first identified morphogens and it remains a benchmark system for studies of gradient formation (5–9). During oogenesis, *bcd* mRNAs are maternally deposited at the anterior pole of the oocyte (10). The Bcd protein, translated upon egg laying, then forms an exponential concentration gradient with its maximum at the anterior pole (11).

Because of the syncytial nature of fly embryos, a simple model, referred to as the synthesis, diffusion, and degradation (SDD) model, was initially proposed for the establishment of the Bcd concentration gradient (11). This model assumes that the morphogen is synthesized at a constant rate at the anterior pole, freely diffuses along the AP axis, and is uniformly degraded across the embryo (3,12,13).

For a first-order kinetics degradation process, the SDD model predicts the formation of a stable exponential gradient within a time comparable to the morphogen lifetime, τ, and with a decay length, λ, controlled by the diffusion coefficient of the morphogen, D. As $\lambda \sim 100$ μm in *Drosophila melanogaster* embryos (11), and as the gradient seems already established 90 min after fertilization (6), one implication of the SDD model is that Bcd should have an effective diffusion coefficient of at least 2 $\mu m^2/s$.

Recently, fluorescence recovery after photobleaching (FRAP) experiments were interpreted as showing that a Bcd-EGFP fusion protein had an apparent diffusion coefficient of ~0.3 $\mu m^2/s$ in the cytoplasm of *Drosophila* embryos (6). This slow mobility represents a serious challenge to the SDD model, because it either means that the Bcd gradient is not yet stabilized after ~90 min (14), or (more radically) that it is not formed by diffusion of the morphogen. This has led to propositions that the Bcd concentration gradient may instead be formed by advective transport (8) or by an underlying mRNA gradient (7). In contrast, recent mobility measurements based on a different approach, fluorescence correlation spectroscopy (FCS), have shown that in zebrafish embryos, the Fgf8 morphogen gradient is formed by diffusion (15).

So do we need to abandon the SDD model for Bicoid? To answer this question, we have revisited the issue of the stability of the Bcd gradient in *D. melanogaster* embryos and measured the mobility of the protein in the cortical cytoplasm using FCS.

To verify when the gradient became stable, we acquired one-photon confocal images of embryos expressing both Bcd-EGFP (6) and a marker for the nuclear envelope, Nup107-mRFP (16), which we used to identify in-focus nuclei (Fig. 1 and see Fig. S1 and Fig. S2 in the Supporting Material). EGFP fluorescence became clearly visible around nuclear cycle 10, and it was then readily observed until nuclear cycle 14. In agreement with previous observations (6,11), the Bcd-EGFP protein accumulated in nuclei during interphase and was distributed according to a seemingly exponential concentration gradient along the AP axis of the embryo (Fig. 1, *A* and *C*). The concentration of fluorescent Bcd-EGFP molecules was estimated using FCS to

Editor: Michael Edidin.

doi: 10.1016/j.bpj.2010.05.031

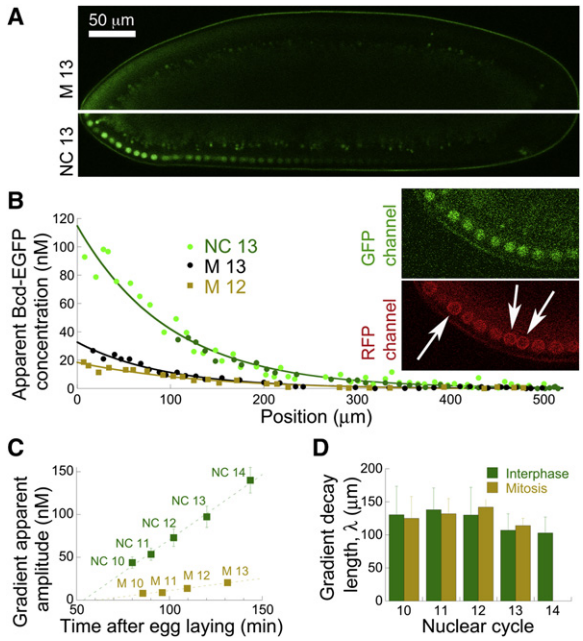

FIGURE 1 (*A*) Bcd-EGFP fluorescence during nuclear cycle 13 (NC 13, *lower panel*) and the ensuing mitosis (M 13, *upper panel*) (average of three confocal images taken 2 μm apart). (*B*) Bcd-EGFP fluorescence gradient for the embryo shown in panel *A*. (*Inset*) Detail of a single confocal image of the embryo in both GFP and RFP channels, with arrows pointing at in-focus nuclei. (*C*) Amplitude and (*D*) decay length of the Bcd-EGFP gradient in interphase nuclei (NC 10–14) and mitotic cytoplasm (M 10–13) (mean $\pm$ SD, $n = 5$).

be ~140 nM in anterior nuclei at the beginning of cycle 14 (see Section E in the Supporting Material). This value was then used as an internal calibration to estimate apparent Bcd-EGFP concentration at different positions in the embryos and during different nuclear cycles from the fluorescence intensity recorded in confocal images (Fig. 1, *C* and *D*). We observed a regular increase in EGFP fluorescence over time with a degree of variability within each cycle (Fig. 1 *D*). Because nuclear EGFP-Bcd concentration varies during interphase, the increase in nuclear fluorescence we observed is difficult to interpret, whereas the linear increase in EGFP fluorescence in the mitotic cytoplasm is a robust observation which indicates that the total amount of fluorescent Bcd-EGFP keeps increasing until at least cycle 14. This increase, however, is likely affected by the slow maturation of the EGFP fluorophore, which may take ~1 h in vivo (17). It is thus difficult to directly relate fluorescence intensities to absolute Bcd concentration and to gradient stability. In contrast to its apparent amplitude, the decay length of the gradient remained stable throughout nuclear cycles 10–14, on average λ ~125 μm, both during mitosis and when considering nuclear Bcd-EGFP in interphase (Fig. 1 *E*). According to the time-dependent interpretation of the SDD model (4), and considering the observed ~20% standard deviation on the value of λ measured during cycles 10–12, the decay length of the gradient will appear stable after ~1.3τ (see Section D in the Supporting Material for details). Therefore, our observation that the decay length of the gradient is stable by cycle 10, 80 min after fertilization, suggests that $\tau < 60$ min.

To understand how the Bcd concentration gradient could be established so quickly, we obtained the mobility of Bcd-EGFP in the anterior cortical cytoplasm of the embryos using single-point FCS and we compared it to the mobility of a control NLS-EGFP fusion protein (18). Measurements were taken in the cortical cytoplasm of the anterior region of embryos during interphases of cycles 12–14. We analyzed the average autocorrelation function obtained for each protein (using $n = 13$ separate FCS measurements for Bcd-EGFP, and $n = 10$ for NLS-EGFP) with different diffusion models (one-, two-, and three-species; simple and anomalous) and with different assumptions about EGFP photophysics (Fig. 2, and see Section E in the Supporting Material). We found that the behavior of Bcd-EGFP in the cortical cytoplasm of the *Drosophila* embryo cannot be accounted for by the diffusion of a single species. The data did not allow clear discrimination between more complex diffusion models, yet all models agreed that the mobility of Bcd-EGFP in the cortical cytoplasm of the embryos corresponds to an average diffusion coefficient lying between 5 and 10 $\mu m^2/s$, with a likely value $D = 7.4 \pm 0.4$ $\mu m^2/s$. The mobility of the control protein NLS-EGFP was approximately threefold larger, with an apparent diffusion coefficient $D = 24 \pm 1$ $\mu m^2/s$.

Our estimate of the average diffusion coefficient of Bcd-EGFP is one-order-of-magnitude larger than the value derived from FRAP measurements performed by Gregor et al. (6) on the same system. Therefore, we sought to obtain an independent assessment of the cytoplasmic mobility of Bcd-EGFP using raster-scanning FRAP experiments (see Section F in the Supporting Material). For all the experimental conditions accessible with our commercial confocal instrument, the measured fluorescence recovery half-time, $\tau_{1/2}$, was comparable to the duration of the photobleaching step, T_P. This indicates that Bcd-EGFP molecules cannot be considered immobile during the photobleaching step, and thus a value for the diffusion coefficient cannot easily

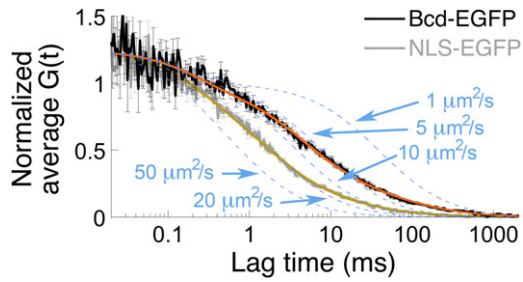

FIGURE 2 Normalized average autocorrelation functions obtained for Bcd-EGFP and NLS-EGFP in the anterior cortical cytoplasm of stage 12–14 embryos (*continuous colored lines*, fit assuming two independent diffusing species). Error bars represent the standard error. (*Dashed blue lines*) Expected autocorrelation functions for one diffusing species and different values of *D*.

be extracted from the data (19). Instead, the value of the recovery half-time can be used to place a lower limit on Bcd-EGFP diffusion coefficient,

$$D \geq 0.224\, w^2/\tau_{1/2} \sim 1\ \mu m^2/s$$

(the lowest value of $\tau_{1/2}$ we measured was 0.21 s, for a radius of the photobleached area w = 0.95 μm). Likewise, because Gregor et al. (6) also found $\tau_{1/2} \sim T_P$, the value $D = 0.3\ \mu m^2/s$ they obtained must be considered as a lower limit for Bcd-EGFP diffusion coefficient rather than an absolute value.

Our data therefore support the fact that Bcd-EGFP is more mobile than previously proposed, with an apparent diffusion coefficient ~7 $\mu m^2/s$. The diffusion coefficient of the 54-kDa endogenous wild-type Bcd should be, if anything, slightly higher than that of the ~80-kDa Bcd-EGFP. It is important to keep in mind that our measurements were limited to cycles 12 and 14, whereas gradient establishment takes place much earlier. In addition, our FCS measurements only provide a snapshot of mobility at the scale of the confocal volume (~1 μm), and do not rule out the possibility that diffusion might be slower at the scale of the whole embryo, which is the scale relevant for gradient formation. However, a strong argument in favor of the similarity of μm- and mm-scale diffusion properties in precellularization *D. melanogaster* embryos is that the diffusion coefficients measured for Bcd-EGFP and NLS-EGFP by FCS are in general agreement with those measured on a much larger scale (by analysis of spatiotemporal concentration profiles) for microinjected 1–150 kDa fluorescent dextrans (20).

The most important implication of this work is that the diffusive motion of Bcd in the cytoplasm is fast enough for its concentration gradient to be established purely by diffusion across the *Drosophila* embryo before the onset of zygotic transcription, which occurs around nuclear cycle 8, ~1 h after egg fertilization. Using the estimate for the diffusion coefficient of cytoplasmic Bcd-EGFP based on our FCS measurements, D ~7 $\mu m^2/s$, and given the observed decay length of the gradient, λ ~125 μm, the SDD model predicts that $\tau \sim \lambda^2/D$ ~40 min. This is in agreement with the observation that the exponential shape of the gradient and its characteristic length already appear stable by the time EGFP fluorescence becomes visible around nuclear cycle 10, ~80 min after fertilization and egg laying. Therefore, our observations show that a mechanism based on morphogen diffusion, as proposed in the SDD model and as observed for Fgf8, is still a plausible alternative for Bcd. Even if processes other than diffusion are important, alternative models for gradient formation will need to include explanations of how these potential other processes would be able to overcome Bcd diffusion.

SUPPORTING MATERIAL

Six sections, five figures, two tables, and three equations are available at http://www.biophysj.org/biophysj/supplemental/S0006-3495(10)00669-7.

ACKNOWLEDGMENTS

We thank Dr. E. Wieschaus for providing *Drosophila* strains, Dr. A. Campos for help with fly maintenance, and Dr. T. Collins, Dr. F. Waharte, and the Imagery platform PICT-Ibisa of the Institut Curie for technical help.

This work was supported by the France-Canada Research Foundation, the Natural Sciences and Engineering Research Council (Canada), and the Centre National de la Recherche Scientifique. C.F. is the recipient of a Canada Research Chair grant. A.P. was supported by the Université Paris Diderot and N.D. by the Institut National de la Santé et de la Recherche Médicale.

REFERENCES and FOOTNOTES

1. Wolpert, L. 1996. One hundred years of positional information. *Trends Genet.* 12:359–364.
2. Crauk, O., and N. Dostatni. 2005. Bicoid determines sharp and precise target gene expression in the *Drosophila* embryo. *Curr. Biol.* 15: 1888–1898.
3. Houchmandzadeh, B., E. Wieschaus, and S. Leibler. 2005. Precise domain specification in the developing *Drosophila* embryo. *Phys. Rev. E Stat. Nonlin. Soft Matter Phys.* 72:061920.
4. Bergmann, S., O. Sandler, …, N. Barkai. 2007. Pre-steady-state decoding of the Bicoid morphogen gradient. *PLoS Biol.* 5:e46.
5. Coppey, M., A. M. Berezhkovskii, …, S. Y. Shvartsman. 2007. Modeling the Bicoid gradient: diffusion and reversible nuclear trapping of a stable protein. *Dev. Biol.* 312:623–630.
6. Gregor, T., E. F. Wieschaus, …, D. W. Tank. 2007. Stability and nuclear dynamics of the Bicoid morphogen gradient. *Cell.* 130:141–152.
7. Spirov, A., K. Fahmy, …, S. Baumgartner. 2009. Formation of the Bicoid morphogen gradient: an mRNA gradient dictates the protein gradient. *Development.* 136:605–614.
8. Hecht, I., W. J. Rappel, and H. Levine. 2009. Determining the scale of the Bicoid morphogen gradient. *Proc. Natl. Acad. Sci. USA.* 106: 1710–1715.
9. Porcher, A., and N. Dostatni. 2010. The Bicoid morphogen system. *Curr. Biol.* 20:R249–R254.
10. Berleth, T., M. Burri, …, C. Nüsslein-Volhard. 1988. The role of localization of Bicoid RNA in organizing the anterior pattern of the *Drosophila* embryo. *EMBO J.* 7:1749–1756.
11. Driever, W., and C. Nüsslein-Volhard. 1988. A gradient of Bicoid protein in *Drosophila* embryos. *Cell.* 54:83–93.
12. Crick, F. 1970. Diffusion in embryogenesis. *Nature.* 225:420–422.
13. Lewis, J., J. M. Slack, and L. Wolpert. 1977. Thresholds in development. *J. Theor. Biol.* 65:579–590.
14. Bergmann, S., Z. Tamari, …, N. Barkai. 2008. Re-examining the stability of the Bicoid morphogen gradient. *Cell.* 132:15–17.
15. Yu, S. R., M. Burkhardt, …, M. Brand. 2009. Fgf8 morphogen gradient forms by a source-sink mechanism with freely diffusing molecules. *Nature.* 461:533–536.
16. Katsani, K. R., R. E. Karess, …, V. Doye. 2008. In vivo dynamics of *Drosophila* nuclear envelope components. *Mol. Biol. Cell.* 19: 3652–3666.
17. Helm, R., A. B. Cubitt, and R. Y. Tsien. 1995. Improved green fluorescence. *Nature.* 373:664–665.
18. Gregor, T., A. P. McGregor, and E. F. Wieschaus. 2008. Shape and function of the Bicoid morphogen gradient in dipteran species with different sized embryos. *Dev. Biol.* 316:350–358.
19. Waharte, F., C. M. Brown, …, F. Amblard. 2005. A two-photon FRAP analysis of the cytoskeleton dynamics in the microvilli of intestinal cells. *Biophys. J.* 88:1467–1478.
20. Gregor, T., W. Bialek, …, E. F. Wieschaus. 2005. Diffusion and scaling during early embryonic pattern formation. *Proc. Natl. Acad. Sci. USA.* 102:18403–18407.